Seismic scaling relation of the 2007 Off Mid Niigata, Japan, earthquake (M_w 6.6) sequence in comparison with two other earthquake (M_w 6.6) sequences

Reiko Tajima and Fumiko Tajima

Department of Earth and Planetary Systems Science, Graduate School of Science, Hiroshima University, 1-3-1 Kagami-yama, Higashi-Hiroshima 739-8526, Japan

(Received November 15, 2007; Revised January 15, 2008; Accepted January 30, 2008; Online published November 18, 2008)

The relationship of seismic moment (M_0) to corner frequency (f_c) of the 2007 Off Mid Niigata prefecture (Chuetsu-oki) earthquake sequence is examined in comparison with that of two other earthquake sequences. The M_0-f_c relation of this sequence ($3.4 \leq M_w \leq 6.6$) is $M_0 \propto f_c^{-3.87}$, which deviates from $M_0 \propto f_c^{-3}$. The relatively large deviation from f_c^{-3} may reflect the influence of fluids identified in tomographic studies around the source region of the tectonic strain concentration. Moreover, the lower f_cs of the small events ($3.4 \leq M_w \leq 3.8$) in this sequence are similar to those of off-main-fault events in the 2004 Mid Niigata prefecture earthquake sequence. The characteristics in the scaling relation may be interpreted in the context of the event locations, which are either on- or off-main faults, and may have implications for the seismogenic conditions.

Key words: The 2007 Off Mid Niigata earthquake, seismic scaling, seismogenic conditions.

1. Introduction

The 16 July 2007 Off Mid Niigata prefecture (Chuetsu-oki) earthquake (OMNE) occurred in the central part of Japan about 40 km northwest of the 23 October 2004 Mid Niigata prefecture earthquake (MNE). Both of the main shocks had an identical moment magnitude (M_w) of 6.6 and a reverse-fault mechanism (see Fig. 1). The Niigata district is located in the region of tectonic strain concentration along the Niigata-Kobe tectonic zone (Sagiya *et al*., 2000). Geological studies indicate that profound surface folding has been developing around the source region since 3.5 Ma, following the extension stage of the Japan Sea (Sato, 1994).

The aftershock areas of the OMNE and MNE extended about 30 km northeast-southwest, and multiplanar faults, including a conjugate set, produced large events of $M_w \geq 5.5$. While the two sequences have common features, the aftershock activity differed in that the OMNE sequence consisted of a small number of aftershocks, whereas the MNE sequence produced many, including six large aftershocks with $M_w \geq 5.5$. Some of the OMNE aftershocks have normal-fault mechanisms that are different from the reverse-fault mechanism of the main shock (Japan Meteorological Agency (JMA), 2007). The dip angle of the OMNE main shock fault plane has been controversial; whether it is a single fault dipping to the northwest or southeast, or a conjugate of two fault mechanisms (dipping northwest and southeast) that moved simultaneously (e.g., Geographical Survey Institute, 2007; Koketsu and Strong Motion Seismology Group, ERI, Unv. Tokyo, 2007; National Research Institute for Earth Science and Disaster Prevention (NIED), 2007).

Izutani (2005) and Tajima and Tajima (2007) indicate that the scaling relationship between seismic moment (M_0) and corner frequency (f_c) of the MNE sequence deviates from $M_0 \propto f_c^{-3}$. In general, the f_c in the source spectrum is essential for estimating the radiated seismic energy (E_R) that characterizes the dynamic rupture properties of an earthquake. However, the source spectra sometimes become more complex than those expected from a typical omega-square (ω^{-2}) model (Brune, 1970) in the vicinity of f_c (Mayeda and Walter, 1996). Tajima and Tajima (2007) report the different M_0-f_c relations between the MNE and the 2005 West Off Fukuoka prefecture earthquake (WOFE) (M_w 6.6) sequences ($3.5 \leq M_w \leq 6.6$) and suggest the variability of scaling relations in individual earthquake sequences.

The present study determines the f_cs of the OMNE and the aftershocks ($3.4 \leq M_w \leq 6.6$) using the spectral ratio method (Tajima and Tajima, 2006, 2007) and compares the scaling relationships among the three earthquake sequences. We take into account the complex tectonic or seismogenic conditions among sequences in this region of tectonic strain concentration.

2. Spectral Ratio Method and Data

Figure 1(a) shows the locations of the main shock and aftershocks of the 2007 OMNE sequence in comparison with the 2004 MNE. The three F-net stations used in this study are also shown. The F-net is the network of broadband velocity seismometers maintained by NIED in Japan. The F-net stations SBT, ASI, and WJM are located at distances of approximately 84, 128, and 141 km from the main shock

Table 1. Source parameter of the 2007 Off Mid Niigata prefecture earthquake sequence.

Origin time (JST)[a]	Latitude[a]	Longitude[a]	Depth[a]	Strike[b]	Dip[b]	Rake[b]	Moment[b]	M_W[b]	Delta[c]	f_c[d]	Variance[e]
y m d h m	deg	deg	km	deg	deg	deg	N m		km	Hz	
2007/07/16,10:13	37.5568	138.6095	16.75	215	49	80	9.30e+18	6.6	—	0.12±0.028	
2007/07/16,15:37	37.5040	138.6445	22.53	219	47	100	3.26e+17	5.6	6.63	0.41±0.067	
2007/07/16,18:58	37.4407	138.4645	21.12	211	41	81	2.95e+14	3.6	18.18	1.62 (1.64)	0.261
2007/07/16,22:55	37.5333	138.5595	17.72	196	42	54	4.21e+14	3.7	5.13	2.10 (2.04)	0.146
2007/07/17,10:26	37.4908	138.5177	18.20	216	31	69	4.91e+14	3.8	10.93	1.14 (1.34)	0.218
2007/07/20,21:54	37.4480	138.5693	19.50	225	60	116	1.61e+14	3.4	12.59	2.04 (2.40)	0.226
2007/07/24,15:51	37.3982	138.5370	18.70	223	50	94	1.43e+14	3.4	18.74	2.70 (2.24)	0.169
2007/07/25,06:52	37.5328	138.7212	24.21	203	41	88	1.18e+16	4.7	10.23	1.10	0.194
2007/08/06,14:53	37.5088	138.5773	13.62	206	47	70	1.86e+14	3.5	6.04	1.88 (1.80)	0.212

[a]After the JMA catalog.

[b]After the NIED F-net event catalog.

[c]Distance from the main shock.

[d]Estimated f_cs. The numbers in the parentheses indicate the f_cs obtained from the spectral ratios with the largest aftershock.

[e]Variance in the grid search for the spectral ratio of the main shock to each smaller aftershock.

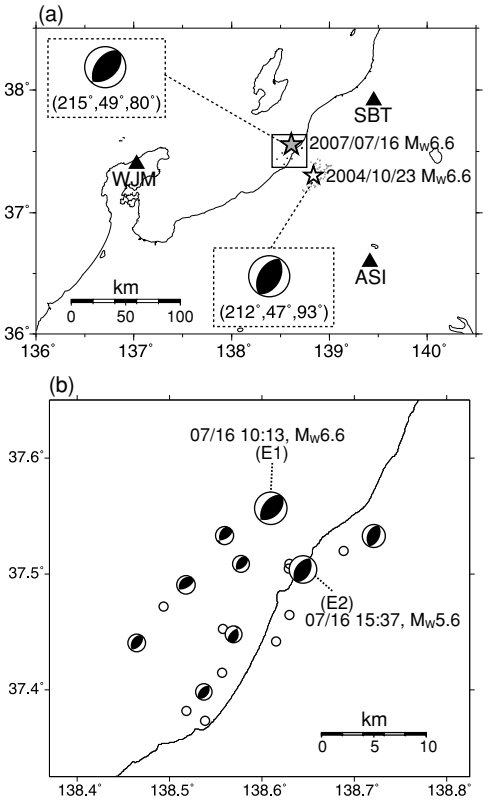

Fig. 1. Distribution of earthquake epicenters and stations used in this study. (a) Locations of the mainshocks (stars) with the focal mechanisms and the aftershocks (small dots) for the 2007 Off Mid Niigata prefecture (Chuetsu-oki) earthquake (OMNE) and 2004 mid Niigata prefecture earthquake (MNE) sequences. Three F-net stations (triangles) used in this study are also shown. (b) Distribution of the main shock (M_w 6.6), largest aftershocks (M_w 5.6), and selected seven aftershocks ($3.5 \leq M_w \leq 4.7$) of the OMNE sequence with the focal mechanisms determined by NIED F-net operation. The hypocenters are provided by JMA.

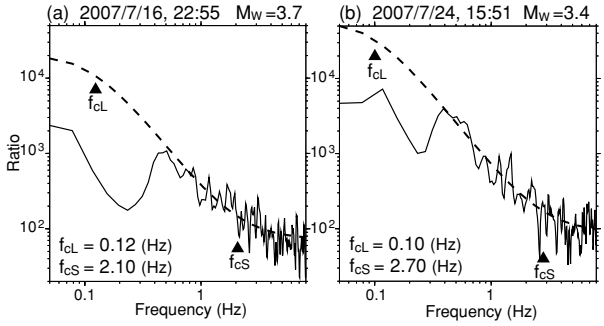

Fig. 2. Example of the spectral ratio fitting and the estimation of corner frequencies (f_cs). The solid lines show the averaged spectral ratios obtained from the observed data. The dashed lines represent the theoretical spectral ratios calculated using Eq. (1). The triangles indicate f_cs of the large and small events. (a) Spectral ratio of the main shock (M_w 6.6) to a 16 July 2007 aftershock (M_w 3.7). (b) Same as (a) but using a 24 July 2007 aftershock (M_w 3.4).

epicenter, respectively.

The f_cs were estimated for the OMNE main shock (M_w 6.6), the largest aftershock (M_w 5.6), and seven small aftershocks ($3.4 \leq M_w \leq 4.7$) of the sequence using the spectral ratio method. Table 1 summarizes the source parameters of the selected events. The M_0s and focal mechanism solutions are determined in the F-net routine operation (Fukuyama *et al*., 1998). Figure 1(b) shows the distribution of events used for this study, with their focal mechanisms. These selected events satisfy the following conditions:

(1) The study period of data is 40 days after the main shock.
(2) The waveform data were recorded at the three common F-net stations (SBT, ASI, and WJM) and have a good signal-to-noise ratio (S/N).
(3) The focal mechanisms are similar to that of the main event, strike = 215°, dip = 49°, rake = 80° (see Fig. 1(b)).

The spectral ratio method used in this study is almost identical to that described in Tajima and Tajima (2006, 2007). The spectral ratio for a pair that consists of a large and a small event (Hough and Kanamori, 2002) is calculated as:

$$\frac{\dot{M}_L(f)}{\dot{M}_S(f)} = \frac{M_{0L}}{\left[1+(f/f_{cL})^2\right]} \Big/ \frac{M_{0S}}{\left[1+(f/f_{cS})^2\right]}. \quad (1)$$

Here, $\dot{M}(f)$, M_0, and f_c are the source spectrum approxi-

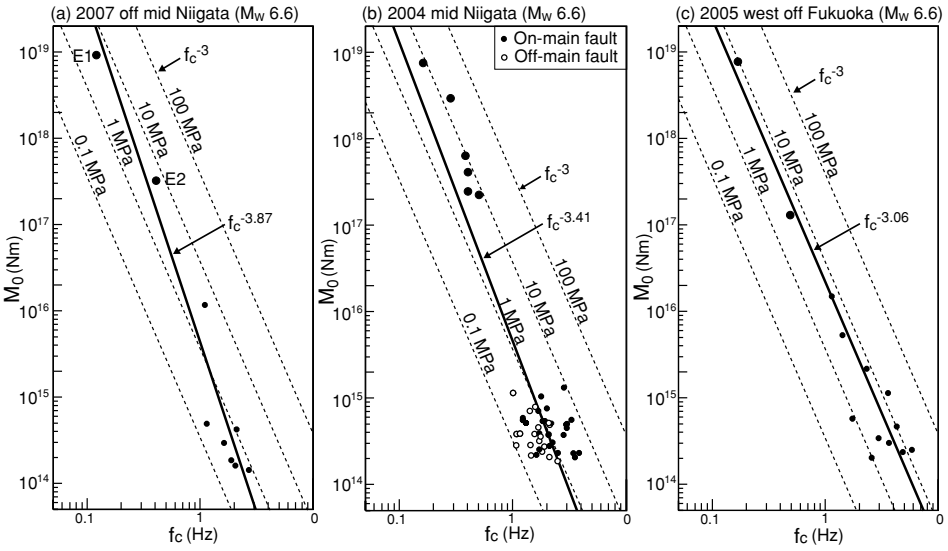

Fig. 3. Comparison of seismic moment (M_0) versus f_c relationship among the OMNE, MNE, and 2005 West Off Fukuoka prefecture earthquake (WOFE) sequences. (a) M_0-f_c relation of the OMNE main shock (E1), large aftershocks (E2), and seven aftershocks in the range of $3.4 \leq M_w \leq 6.6$. The solid line shows the best-fit least squares relations, $M_0 \propto f_c^{-3.87}$. (b) and (c) M_0-f_c relation of the MNE sequence ($M_0 \propto f_c^{-3.41}$) and that of the WOFE sequences ($M_0 \propto f_c^{-3.06}$) derived from Tajima and Tajima (2007), respectively. The solid and open circles in (b) denote plots of the on- and off-main fault events in Fig. 4(b). Four thin dotted lines show the relations of $M_0 \propto f_c^{-3}$ for constant stress drops 0.1, 1, 10, and 100 MPa.

mated by an ω^{-2} model, seismic moment, and corner frequency, respectively. The suffixes L and S are for the large and small events, respectively. If $\dot{M}_L(f)$ is the spectrum of the main shock or the largest aftershock, $\dot{M}_S(f)$ is the spectrum of one of the selected aftershocks or one of those except for the aftershock with M_w 4.7, respectively. We calculate spectra using the waveforms of time window 9 s (1 s before the first arrival plus 8 s), so that we use only P waves (vertical components) throughout the analysis. The left-hand side of Eq. (1) is replaced by $\sum_{i=1}^{3} \dot{M}_L(f) \big/ \sum_{i=1}^{3} \dot{M}_S(f)$, in which the spectra of numerator and denominator are summed up at the three common stations, respectively. When the ratios are taken, the structural effects and attenuation along the different propagation paths and the radiation pattern are averaged, and the propagation path effects are removed.

The spectral ratios thus calculated can be used to determine the corner frequencies f_{cL} and f_{cS} for the large and small events by a grid search minimizing the least-squares errors. However, as the spectral ratios at the frequency band below about 0.5 Hz are not reliable due to the low S/N of small events (see Fig. 2), f_cs are estimated using a grid search for a theoretical spectral ratios fitted to an observed ones in the frequency range from 0.8 to 7 Hz, where the S/N is viable. Since the f_{cL} of the main shock or the largest aftershock is estimated for each of the small aftershocks in the denominator, the f_{cL} is calculated by averaging the f_{cL}s derived from the spectral ratios.

3. Results and Comparison

Figure 2 shows examples of the observed (solid line) and the best-fit theoretical (dashed line) spectral ratio of the main shock to one of the aftershocks of the OMNE sequence. The estimated f_cs (triangles) are also shown. The f_{cL}s of the main shock and largest aftershock are 0.12 ± 0.028 and 0.41 ± 0.067 Hz, respectively. The f_{cS}s for the smaller aftershocks obtained from the spectral ratios with the main shock were determined in the range from 1.1 to 2.7 Hz (see the f_c in Table 1). The relationship between M_0 and f_c is shown in Fig. 3(a). We showed variance in the grid search ($0.8 \leq f \leq 7$ Hz) for the spectral ratio of the main shock to each smaller aftershock in Table 1 to evaluate the uncertainty for the f_{cS} determinations. We also showed the f_{cS}s for six small aftershocks (except an aftershock of 25 July 2007; M_w 4.7) using the spectral ratio with the largest aftershock shown in parentheses in Table 1. The results are basically same as those obtained with the main shock. This evaluation indicates the stable estimation of f_{cS}s.

The range of static stress drop ($\Delta\sigma_S$) which can be estimated assuming a circular fault model (Brune, 1970; Hanks and Wyss, 1972) is indicated (thin dotted lines) for 0.1, 1, 10, and 100 MPa. The M_0-f_c relation of larger events ($4.7 \leq M_w \leq 6.6$) shows a range of $\Delta\sigma_S$ from ~1 to 10 MPa while that of small events ($3.4 \leq M_w \leq 3.8$) shows $\Delta\sigma_S$ from ~0.1 to 1 MPa along a straight line, $M_0 \propto f_c^{-3}$ (given a constant $\Delta\sigma_S$) (Fig. 3(a)). The $\Delta\sigma_S$ of small events are about an order of magnitude smaller than those of the larger events. The best-fit line determined in a least-squares sense is $M_0 \propto f_c^{-3.87}$ in the M_w range from 3.4 to 6.6.

The M_0-f_c relations of the MNE and WOFE sequences ($3.5 \leq M_w \leq 6.6$) derived by Tajima and Tajima (2007) are compared with that of the OMNE (Fig. 3(b, c)). The M_0-f_c relation of the MNE sequence is $M_0 \propto f_c^{-3.41}$ which also deviates from $M_0 \propto f_c^{-3}$ (Fig. 3(b)) while the best fit line for the WOFE sequence ($M_0 \propto f_c^{-3.06}$) is close to $M_0 \propto f_c^{-3}$ (Fig. 3(c)).

4. Discussion and Summary

We carried out a spectral ratio analysis using the 2007 OMNE sequence that occurred in a similar tectonic region to the 2004 MNE sequence. The M_0-f_c relation estimated for the OMNE sequence in the range of $3.4 \leq M_w \leq 6.6$ is

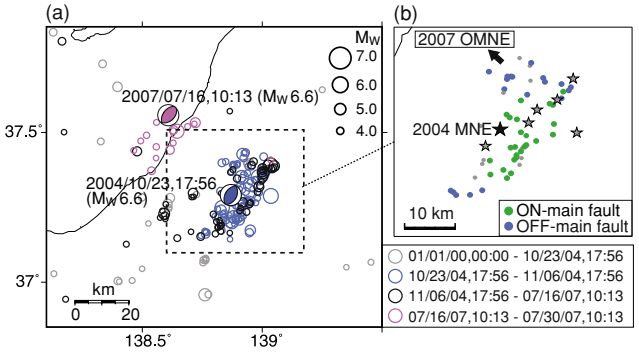

Fig. 4. Epicentral distribution around the studied area. (a) Distribution of event epicenters ($M_w \geq 3.5$) around the OMNE and MNE sequences during the period from 1 January 2000 to 30 July 2007 (determined by JMA). Blue and pink open circles that correspond to the M_ws denote the earthquake epicenters that occurred during two weeks after the MNE and OMNE mainshocks, respectively. (b) Aftershock distribution of the MNE sequence analyzed by Tajima and Tajima (2007). This area corresponds to that enclosed by dashed rectangle in (a). A black star and six gray stars denote the main shock and large aftershock ($M_w \geq 5.5$), respectively. The green and blue solid circles show the aftershocks occurred on and off the main faults, respectively. The epicenters are relocated by Shibutani *et al*. (2005).

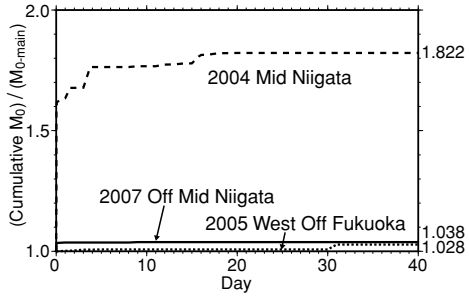

Fig. 5. Cumulative M_0 of events with $M_w \geq 3.5$ during 40 days after the mainshock normalized by the mainshock M_0. Solid, dashed, and dotted lines denote the 2007 MNPE, 2004 MNPE, and 2005 WOFE (M_w 6.6) sequences, respectively.

$M_0 \propto f_c^{-3.87}$, which deviates from $M_0 \propto f_c^{-3}$ (Fig. 3(a)). The M_0-f_c relation of the MNE sequence estimated by Tajima and Tajima (2007) also deviates from $M_0 \propto f_c^{-3}$ (Fig. 3(b)). As described above, both of the source areas are located in the region characterized by active thrusting and folding, and multiplanar faults.

The seismic tomography model that includes the areas of the OMNE and MNE sequences (Okada *et al*., 2006; Nakajima and Hasegawa, 2008) shows low-velocity anomalies beneath the hypocentral region of both. These suggest that the low-velocity areas represent the distribution of water rising from a greater depth due to upwelling flow within the mantle wedge. Closer examinations of the tomography model indicate that the MNE aftershocks along the main shock rupture zone were distributed around the boundary between the high- and low-velocity anomaly zones, and some parts of other fault planes that were imaged as low-velocity anomaly zones (Kato *et al*., 2006; Korenaga *et al*., 2005; Okada *et al*., 2005).

These observations may be related to an episode of fault-valve behavior due to upwardly migrating overpressured fluids during the main shock, as was pointed out for the MNE (Sibson, 2007). Higher pore pressure lowers effective friction and may be expected to lead to a higher E_R during faulting. The f_cs (or $\Delta\sigma_S$s) of the main shocks of the OMNE and MNE, including the large immediate aftershocks ($M_w \geq 5.5$), are close to that of the WOFE. After fluid discharge, the fluids and lower pore pressures could result in lower E_Rs (or f_cs) of smaller aftershocks. The fluids identified in tomographic studies (Kato *et al*., 2006; Korenaga *et al*., 2005; Okada *et al*., 2005, 2006) around the OMNE and MNE source regions may have influenced the more complex fault ruptures more than that of the WOFE. The possible heterogeneous distribution of fluids may be responsible for the deviation from the standard model in the scaling relations.

The moment rate functions of the OMNE and MNE main shocks show relatively long source durations, i.e., approximately 15 s and 11 s, respectively, and are more complex than a simple triangle (e.g., Yagi, 2005; preliminary results: http://www.geo.tsukuba.ac.jp/press_HP/yagi/EQ/2007niigata/ by Yagi, 2007). On the other hand, the moment rate function of the WOFE is approximated by a simple triangle with a duration of ~4 s (Horikawa, 2006). The characteristics of the source time functions as well as the different M_0-f_c relations may be interpreted in terms of the relative fault maturity, as suggested by Tajima and Tajima (2007). The model of relative fault maturity is inferred from the E_R and rupture speed of the main shocks (Choy and Kirby, 2004; Choy *et al*., 2006).

The deviation of the M_0-f_c relation of the OMNE sequence ($f_c^{-3.87}$) from $M_0 \propto f_c^{-3}$ is larger than that of the MNE sequence ($f_c^{-3.41}$), which indicates there is variation in the scaling relation even for similar tectonic conditions. Figure 4(a) shows the event distribution ($M_w \geq 3.5$) around the two source areas during the period from 1 January 2000 to 30 July 2007 as determined by JMA. The seismic activity near the OMNE sequence had been quiet before the main shock (see gray, blue, and black open circles in Fig. 4(a)). Moreover, as shown in Fig. 5, the cumulative M_0 release by the OMNE aftershocks ($M_w \geq 3.5$) during the 40-day period was only 3.8% of the main shock whereas that of the MNE sequence was about 82% of the main shock. The OMNE aftershock activity is low compared to that of the MNE and comparable to that of the WOFE.

Figure 4(b) shows the distribution of the MNE aftershocks which are mainly distributed on the southeastern side of the main shock fault (Tajima and Tajima, 2007; see blue open circles in Fig. 4(a)). However, the aftershocks that occurred near the northern boundary of the aftershock area are located off the main fault (see the epicenters denoted by blue, solid circles in Fig. 4(b)). The f_cs of the off-main-fault events are plotted as open circles in Fig. 3(b).

The characteristics of lower f_cs or $\Delta\sigma_S$s for the small events of the OMNE sequence in $3.4 \leq M_w \leq 3.8$ (Fig. 3(a)) are similar to those of the off-main-fault events in the MNE sequence (open circles in Fig. 3(b)). The variation of f_c (or E_R) observed for the small events may be related to stress redistribution in a complex fault system during the earthquake sequence. Considering the partition of the total

seismic energy (E), if the fracture energy (E_G) (see Mori *et al*., 2003; Venkataraman and Kanamari, 2004) varies in a complex structure, the energy left for seismic radiation (E_R) could also vary. The lower f_{cS}s for the OMNE sequence suggest lower E_R (or higher E_G) that is reflected in the lower aftershock activity (see Fig. 5) and the indistinct main shock fault. The OMNE source rupture seems to be composed of a conjugate of two mechanisms. The difference of the scaling relation for the small events can be interpreted in context of the event locations, i.e., whether they are on or off the main faults. The comparison of the scaling relationship between the on- and off-main-fault events seems to have implications for seismogenic conditions, probably reflecting different rupture processes of the main event, and aftershocks, perhaps with fluids around the source area.

Acknowledgments. We thank T. Shibutani and his colleagues at the Disaster Prevention Research Institute, Kyoto University for permitting us to use their relocated event catalog of the 2004 Mid Niigata prefecture earthquake. We also thank K. Yomogida, Y. Izutani, and P. Hellweg for helpful comments. We used the event catalogs assembled by JMA and NIED F-net and waveform data from the F-net. The figures were prepared using the Generic Mapping Tools by Wessel and Smith (1995). This study was partially supported by a Research Fellowship for Young Scientists no. 19·4077 (for RT) and a Grant-in-Aid for Scientific Research no. 16340130 (for FT) from the Japan Society for the Promotion of Science.

References

Brune, J., Tectonic stress and the spectra of seismic shear waves from earthquakes, *J. Geophys. Res*., **75**, 4997–5009, 1970.

Choy, G. L. and S. H. Kirby, Apparent stress, fault maturity and seismic hazard for normal-fault earthquakes at subduction zones, *Geophys. J. Int*., **159**, 991–1012, 2004.

Choy, G. L., A. McGarr, S. H. Kirby, and J. L. Boatwright, An overview of the global variability in radiated energy and apparent stress, in *Geophysical Monograph Series*, edited by R. Abercrombie, A. McGarr, H. Kanamori and G. D. Toro, **170**, 43–57, 2006.

Fukuyama, E., M. Ishida, D. S. Dreger, and H. Kawai, Automated seismic moment tensor determination by using on-line broadband seismic waveforms, *Zisin, second ser.*, **51**, 149–156, 1998 (in Japanese with an English abstract).

Geographical Survey Institute (Analysis group for crustal deformation of the Chuetsu-oki earthquake), Crustal deformation and fault model associated with the Niigataken Chuetsu-oki earthquake in 2007 (part 1), *Abstract for 2007 Fall Meeting for the Seismological Society of Japan*, A11-02, 2007 (in Japanese).

Hanks, T. C. and M. Wyss, The use of body wave spectra in the determination of seismic source parameters, *Bull. Seismol. Soc. Am*., **62**, 561–589, 1972.

Horikawa, H., Rupture process of the 2005 West Off Fukuoka Prefecture, Japan, earthquake, *Earth Planets Space*, **58**, 87–92, 2006.

Hough, S. E. and H. Kanamori, Source Properties of Earthquakes near the Salton Sea Triggered by the 16 October 1999 M 7.1 Hector Mine, California, Earthquake. *Bull. Seismol. Soc. Am*., **92**, 1281–1289, 2002.

Izutani, Y., Radiated energy from the mid Niigata, Japan, earthquake of October 23, 2004, and its aftershocks, *Geophys. Res. Lett*., **32**, L21313, doi:10.1029/2005GL024116, 2005.

Japan Meteorological Agency (Seismological and Volcanological Department), Outline of the Niigataken Chuetsu-oki Earthquake in 2007, *Abstract for 2007 Fall Meeting for the Seismological Society of Japan*, A11-01, 2007 (in Japanese).

Kato, A., S. Sakai, N. Hirata, E. Kurashimo, T. Iidaka, T. Iwasaki, and T. Kanazawa, Imaging the seismic structure and stress field in the source region of the 2004 mid-Niigata prefecture earthquake: Structural zones of weakness and seismogenic stress concentration by ductile flow, *J. Geophys. Res*., **111**, B08308, doi:10.1029/2005JB004016, 2006.

Koketsu, K. and Strong Motion Seismology Group, Earthquake Research Institute, University of Tokyo, Source process and strong ground motion of the 2007 Chuetsu-oki earthquake, *Abstract for 2007 Fall Meeting for the Seismological Society of Japan*, A11-04, 2007 (in Japanese).

Korenaga, M., S. Matsumoto, Y. Iio, T. Matsushima, K. Uehira, and T. Shibutani, Three dimensional velocity structure around aftershock area of the 2004 mid Niigata prefecture earthquake (M 6.8) by the Double-Difference tomography, *Earth Planets Space*, **57**, 429–433, 2005.

Mayeda, K. and W. R. Walter, Moment, energy, stress drop, and source spectra of western United States earthquakes from regional coda envelopes, *J. Geophys. Res*., **101**, 11195–11208, 1996.

Mori, J., R. E Abercrombie, and H. Kanamori, Stress drops and radiated energies of the 1994 Northridge, California, earthquake, *J. Geophys. Res*., **108**, 2545–2558, 2003.

Nakajima, J. and A. Hasegawa, Existence of low-velocity zones under the source areas of the 2004 Chuetsu and 2007 Chuetsu-oki earthquakes inferred from travel-time tomography, *Earth Planets Space*, **60**, this issue, 1127–1130, 2008.

National Research Institute for Earth Science and Disaster Prevention (Research Center), Report on the 2007 Niigata-ken Chuetsu-oki earthquake based on the NIED seismograph networks, *Abstract for 2007 Fall Meeting for the Seismological Society of Japan*, A11-03, 2007 (in Japanese).

Okada, T., N. Umino, T. Matsuzawa, J. Nakajima, N. Uchida, T. Nakayama, S. Hirahara, T. Sato, S. Hori, T. Kono, Y. Yabe, K. Ariyoshi, S. Gamage, J. Shimizu, J. Suganomata, S. Kita, S. Yui, M. Arao, S. Hondo, T. Mizukami, H. Tsushima, T. Yaginuma, A. Hasegawa, Y. Asano, H. Zhang, and C. Thurber, Aftershock distribution and 3D seismic velocity structure in and around the focal area of the 2004 mid Niigata prefecture earthquake obtained by applying double-difference tomography to dense temporary seismic network data, *Earth Planets Space*, **57**, 435–440, 2005.

Okada, T., T. Yaginuma, N. Umino, T. Matsuzawa, A. Hasegawa, H. Zhang, and C. Thurber, Detailed imaging of the fault planes of the 2004 Niigata-Chuetsu, central Japan, earthquake sequence by double-difference tomography, *Earth Planet. Sci. Lett*., **244**, 32–43, 2006.

Sagiya, T., S. Miyazaki, and T. Tada, Continuous GPS array and present-day crustal deformation of Japan, *Pure Appl. Geophys*., **157**, 2303–2322, 2000.

Sato, H., The relationship between late Cenozoic tectonic events and stress field and basin development in northeast Japan, *J. Geophys. Res*., **99**, 22,261– 22,274, 1994.

Shibutani, T., Y. Iio, S. Matsumoto, H. Katao, T. Matsushima, S. Ohmi, F. Takeuchi, K. Uehira, K. Nishigami, B. Enescu, I. Hirose, Y. Kano, Y. Kohno, M. Korenaga, Y. Mamada, M. Miyazawa, K. Tatsumi, T. Ueno, H. Wada, and Y. Yukutake, Aftershock distribution of the 2004 Mid Niigata prefecture earthquake derived from a combined analysis of temporary online observations and permanent observations, *Earth Planets Space*, **57**, 545–549, 2005.

Sibson, R. H., An episode of fault-valve behavior during compressional inversion?—The 2004 M_J 6.8 Mid-Niigata Prefecture, Japan earthquake sequence, *Earth Planet. Sci. Lett*., **257**, 188–199, 2007.

Tajima, R. and F. Tajima, The 2004 Mid Niigata prefecture earthquake: characterization of the aftershock area using a spectral ratio analysis, *Zisin, second ser.*, **58**, 445–455, 2006 (in Japanese with an English abstract).

Tajima, R. and F. Tajima, Seismic scaling relations and aftershock activity from the sequences of the 2004 mid Niigata and the 2005 west off Fukuoka earthquakes (M_w 6.6) in Japan, *J. Geophys. Res*., **112**, B10302, doi:10.1029/2007JB004941, 2007.

Venkatarman, A. and H. Kanamori, Observational constraints on the fracture energy of subduction zone earthquakes, *J. Geophys. Res*., **109**, B05302, doi:10.1029/2003JB002549, 2004.

Wessel, P. and W. H. F. Smith, New version of the Generic Mapping Tools released, *EOS Trans., AGU*, **76**, 329, 1995.

Yagi, Y., Source process of the 2004 Mid Niigata prefecture earthquake obtained by joint inversion of near-field and teleseismic, *Abstract for the 2005 Joint Meeting for Earth and Planetary Science, Japan*, S101-P001, 2005 (in Japanese with an English abstract).

R. Tajima (e-mail: re-ko-is-loving-it@hiroshima-u.ac.jp) and F. Tajima